

Phenomenology of retained refractoriness: On semi-memristive discrete media

Andrew Adamatzky¹ and Leon O. Chua²

¹ *University of the West of England, Bristol, UK*
andrew.adamatzky@uwe.ac.uk

² *University of California at Berkeley, Berkeley, USA*
chua@eecs.berkeley.edu

Abstract

We study two-dimensional cellular automata, each cell takes three states: resting, excited and refractory. A resting cell excites if number of excited neighbours lies in a certain interval (excitation interval). An excited cell become refractory independently on states of its neighbours. A refractory cell returns to a resting state only if the number of excited neighbours belong to recovery interval. The model is an excitable cellular automaton abstraction of a spatially extended semi-memristive medium where a cell's resting state symbolises low-resistance and refractory state high-resistance. The medium is *semi*-memristive because only transition from high- to low-resistance is controlled by density of local excitation. We present phenomenological classification of the automata behaviour for all possible excitation intervals and recovery intervals. We describe eleven classes of cellular automata with retained refractoriness based on criteria of space-filling ratio, morphological and generative diversity, and types of travelling localisations.

Keywords: cellular automaton, excitable medium, space-time dynamics

1. Introduction

The memristor (a passive resistor with memory) is a device whose resistance changes depending on the polarity and magnitude of a voltage applied to the device's terminals and the duration of this voltage's application. Its existence was theoretically postulated by Leon Chua in 1971 based on symmetry in integral variations of Ohms laws [7, 8, 9]. The memristor is characterised by a non-linear relationship between the charge and the flux; this relationship can be generalised

to any two-terminal device in which resistance depends on the internal state of the system [8]. The memristor cannot be implemented using the three other passive circuit elements — resistor, capacitor and inductor — therefore the memristor is an atomic element of electronic circuitry [7, 8, 9]. Using memristors one can achieve circuit functionalities that it is not possible to establish with resistors, capacitors and inductors, therefore the memristor is of great pragmatic usefulness. The first experimental prototypes of memristors are reported in [18, 10, 20]. Potential unique applications of memristors are in spintronic devices, ultra-dense information storage, neuromorphic circuits, and programmable electronics [17].

Despite explosive growth of results in memristor studies there is still a few (if any!) findings on phenomenology of spatially extended non-linear media with hundreds of thousands of locally connected memristors. We attempt to fill the gap and develop a minimalistic model of a discrete memristive medium. The only — so far — approaches to develop cellular automata model of a memristive medium are Itoh-Chua memristor cellular automata, where cellular automaton lattice is actually designed of memristors [13], and Adamatzky-Chua model of memristive cellular automata based on structurally-dynamic cellular automata [6]. Both models imitate memristive properties of links, connections between cells of automata arrays but not the cells themselves. In this paper we explore the scenario when link between cells are always 'conductive' but cells themselves can take non-conductive (refractory) states.

We define semi-memristive automata, or excitable cellular automata with retained refractoriness, in Sect. 2. Section 2.5 presents grouping of cell-state transition functions into eleven classes. Hierarchies of classes based on their morphological diversity, space-filling ratio and expressiveness are constructed in Sect. 3. In Sect. 4 we overview a 'zoo' of travelling localizations observed in simulated cellular automata and exemplify interactions between the localizations. Overview of the results is provided in Sect. 5.

2. Definitions and methods

2.1. Semi-memristive automaton

A cellular automaton \mathcal{A} is an orthogonal array of uniform finite-state machines, or cells. Each cell takes the finite number of states and updates its states in discrete time depending on states of its closest neighbours. All cells update their states simultaneously by the same rule. We consider eight-cell neighbourhood and three cell-states: resting \circ , excited $+$, and refractory $-$. Let $u(x) = \{y : |x - y|_{L^\infty} = 1\}$ be a neighbourhood of cell x . Let $\sigma_x^t = \sum_{y \in u(x)} \chi(y^t, +)$ be the sum

of excited neighbours of cell x at time step t , where $\chi(y^t, +) = 1$ if $y^t = +$ and $\chi(y^t, +) = 0$ otherwise. Let $\Theta = [\theta_1, \theta_2]$, $1 \leq \theta_1 \leq \theta_2 \leq 8$, be an excitation interval, and $\Phi = [\phi_1, \phi_2]$, $1 \leq \phi_1 \leq \phi_2 \leq 8$, be a recovery interval. A cell x updates its state by the following rule:

$$x^{t+1} = \begin{cases} +, & \text{if } x^t = \circ \text{ and } \sigma_x^t \in \Theta \\ -, & \text{if } x^t = + \\ \circ, & \text{if } (x^t = \circ \text{ and } \sigma_x^t \notin \Theta) \text{ or } (x^t = - \text{ and } \sigma_x^t \in \Phi) \end{cases}$$

A resting cell becomes excited if the number of its excited neighbours lies in the interval Θ . An excited cell takes refractory state unconditionally. A refractory cell returns to its resting state if number of its excited neighbours lie in the interval Φ .

In computer simulations we consider $\theta_1 = 1$ or 2 and $\theta_1 \leq \theta_2 \leq 8$; there is no point to consider $\theta_1 > 2$ because for such lower boundary of excitation interval most excitation patterns quickly extinct. We adopt the same boundaries of recovery interval Φ : $\phi_1 = 1, 2$ and $\phi_1 \leq \phi_2 \leq 8$. Further we refer to excitation and retention of refractoriness functions as $\mathcal{M}(\theta_1, \theta_2, \phi_1, \phi_2)$.

2.2. Why semi-memristive?

Why do we call the automaton described above a *semi-memristive* automaton? Because we assume that the refractory state symbolises high-resistivity, or non-conductivity. A refractory cell can not be excited whatever number of excited neighbours it has, therefore it can not 'conduct' excitation. In a fully memristive automaton both transitions from excited to refractory and from refractory to resting must be controlled by a local excitation density. In the semi-memristive automaton, the transition from excited to refractory is unconditional and happens independently of a local excitation density but the transition from a refractory state to resting state depends on a local excitation density.

2.3. Experiments

We experiment with cellular automaton array of $n \times n$ cells, $n = 500$, and absorbing boundary conditions. While testing automata's response to external stimulation we use point-wise and D -stimulation (a spatially extended stimulation in a disc). By point-wise stimulation we mean excitation of one cell (for functions, where $\theta_1 = 1$) or two neighbouring cells (for functions, where $\theta_1 = 2$) of elsewhere resting cellular array. The D -stimulation is implemented as follows. Let D -disc be a set of cells which lie at distance not more than r from the centre

$(n/2, n/2)$ of the cellular array. When undertaking D -stimulation we assign excited state to a cell of D with probability 0.1. In computer experiments we used $r = 100$.

2.4. Characteristics used for classification

To classify morphology of configurations generated by functions $\mathcal{M}(\theta_1, \theta_2, \phi_1, \phi_2)$, $\theta_1 = 1, 2$, $\theta_1 \leq \theta_2 \leq 8$, $\phi_1 \leq \phi_2 \leq 8$, we D -stimulate cellular automaton lattices, and subdivided them into classes by visually detected likeness of excitation and refractory patterns generated and based on the following characteristics:

- *Space-filling ratio.* Let automaton of $n \times n$ cells being D -stimulated with disc radius r , then space-filling ratio is a ratio of non-resting cells in configuration recorded at time step $n - r$ (i.e. when front of propagating disturbance just reaches edge of the automaton array) to the size of array n^2 .
- *Morphological diversity* is the number of proportion of different neighbourhood configurations. It is evaluated using Shannon entropy and Simpson's index. Let $W = \{\circ, +, -\}$ be a set of all possible configurations of a 9-cell neighbourhood $w(x) = u(x) \cup x$, $x \in \mathbf{L}$. Let c be a configuration of automaton, we calculate number of non-resting configurations as $\eta = \sum_{x \in \mathbf{L}} \varepsilon(x)$, where $\varepsilon(x) = 0$ if for every resting x all its neighbours are resting, and $\varepsilon(x) = 1$ otherwise. The Shannon entropy is calculated as $-\sum_{w \in W} (v(w)/\eta) \cdot \ln(v(w)/\eta)$, where $v(w)$ is a number of times the neighbourhood configuration w is found in automaton configuration c . Simpson's index is calculated as $1 - \sum_{w \in W} (v(w)/\eta)^2$.
- *Generative diversity* is a diversity of a configuration developed from a point-wise excitation.
- *Expressiveness* of a function is calculated as the Shannon entropy divided by space-filling ratio. Generative expressiveness is the expressiveness calculated after point-wise stimulation.
- *Power of a class* is the number of functions in this class.
- *Ratios of excited and refractory states* are calculated as $n^{-2} \sum_{x \in \mathbf{L}} \chi(x^t, +)$ and $n^{-2} \sum_{x \in \mathbf{L}} \chi(x^t, -)$, where $\chi(a, b) = 1$ if $a = b$, and $\chi(a, b) = 0$ otherwise.

2.5. Classes

We separate functions $\mathcal{M}(\theta_1, \theta_2, \phi_1, \phi_2)$ into eleven classes, characterise morphology of configurations, generated by automata from each class, and provide details on membership of each class.

2.6. Class C_1

D -stimulation gives birth to propagating quasi-chaotic pattern of excited and refractory states, the pattern fills the automaton array (Fig. 1a). A front of the pattern is comprised of branching localised excitations, which periodically merge in a single excitation wave-front; the pattern is almost isotropic with slight indentations along north-south and west-east axis. Excited and refractory states are exhibited equally in patterns generated by automata on class C_1 (Fig. 2, C_1). The class C_1 is comprised of 27 functions: $\mathcal{M}(111a)$, $a = 1, \dots, 8$; $\mathcal{M}(112a)$, $a = 3, \dots, 8$; $\mathcal{M}(121a)$, $a = 2, \dots, 8$; $\mathcal{M}(122a)$, $a = 3, \dots, 8$.

2.7. Class C_2

D -stimulation leads to propagating quasi-chaotic pattern with domination of refractory states. The pattern fills the automaton array (Fig. 1b). The pattern's propagating front is comprised of travelling localizations, which branch periodically. Excited localizations travelling along north-west-south-east and north-east-south-west axis leave a distinctive trail of refractory states (Fig. 1b). There is a tail of gradually extinct excitations. These spatially extended excitations collapse into localised oscillating localizations, most of which extinguish with time (Fig. 2, C_2). The class C_2 has three functions $\mathcal{M}(1122)$, $\mathcal{M}(1211)$, $\mathcal{M}(1222)$.

2.8. Class C_3

Initial random stimulation leads to formation of a single circular excitation wave, followed by trains of excitation waves travelling north-west, north-east, south-west and south-east. The wave-trains are followed by discoidal growing quasi-random pattern of excited and refractory states (Fig. 1c). North, south, east and west domains of cellular array lying between the growing patterns are filled entirely with refractory states. These refractory domains contribute towards slight prevalence of refractory states (Fig. 2, C_3). The class C_3 has eight functions $\mathcal{M}(1a1b)$, $a = 3, \dots, 6$, $b = 1, 2$.

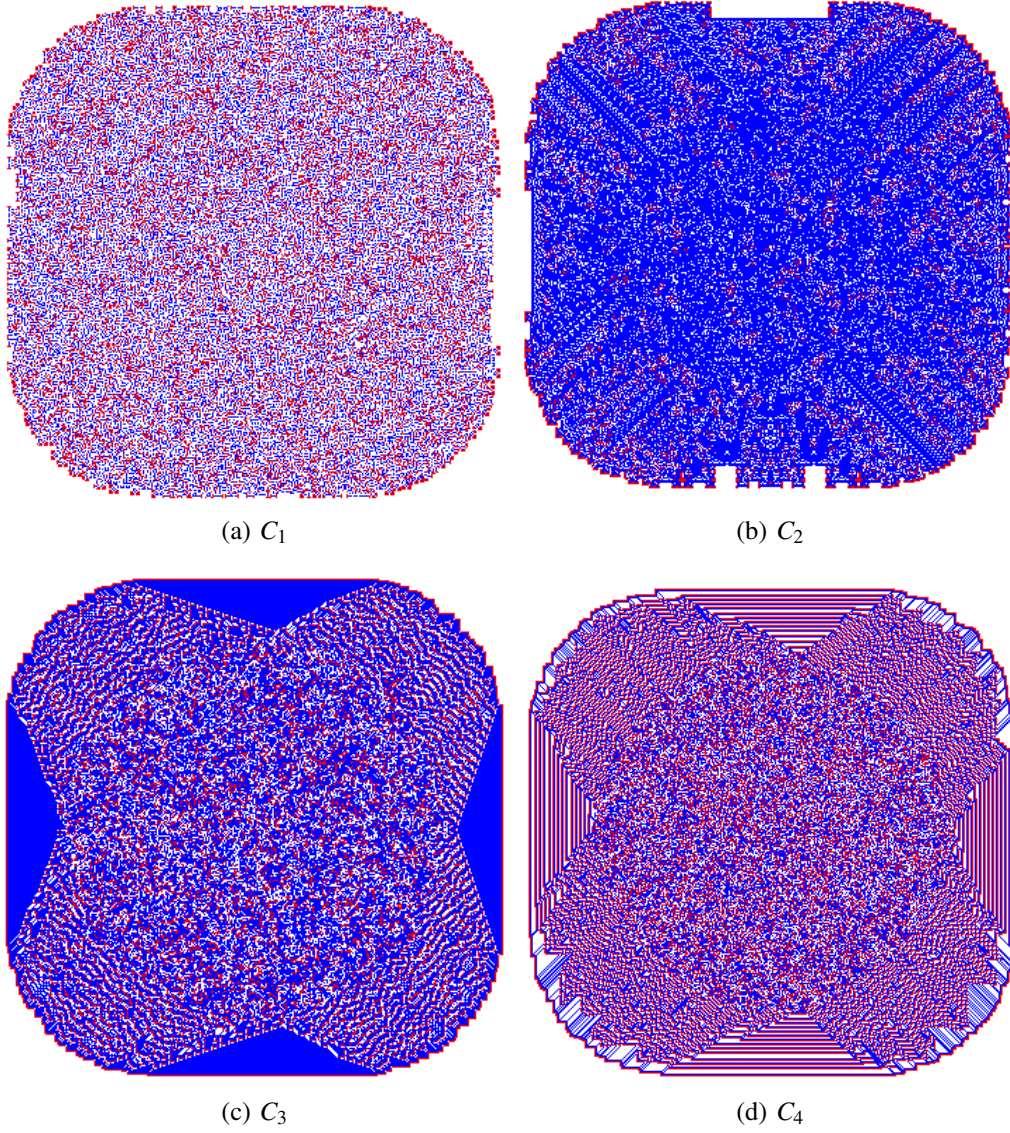


Figure 1: Exemplars of configurations generated by functions from classes $C_1 \dots C_4$ with D -stimulation. Excited cells are red (light grey), refractory cells are blue (dark grey) and resting cells are white.

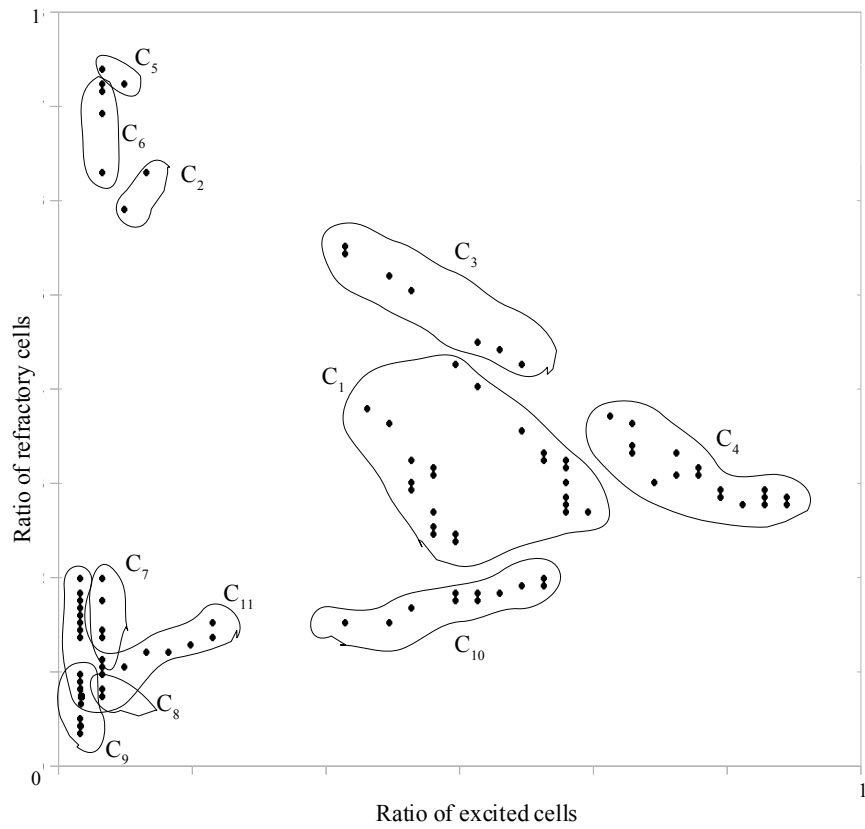


Figure 2: Ratio of excited states to resting states vs ratio of refractory states to resting states in configurations developed by a cellular automaton with retained refractoriness with *D*-stimulation.

2.9. Class C_4

The D -stimulated automata response is characterised by a single circular excitation wave, which encapsulates wave trains propagating north-west, north-east, south-west and south-east, and envelopes of wave-fronts travelling north, east, south and west (Fig. 1d)). The wave envelopes in C_4 occupying the same space domains are refractory domains in C_3 . This is why a cluster of C_4 functions is positioned symmetrically to cluster of C_3 functions with respect to the diagonal of equal ratios of excited and refractory states in Fig. 2. The class C_4 has 48 functions $\mathcal{M}(1abc)$, $a = 3, \dots, 6$, $b = 1, 2$, $c = 3, \dots, 8$.

2.10. Classes C_5 and C_6

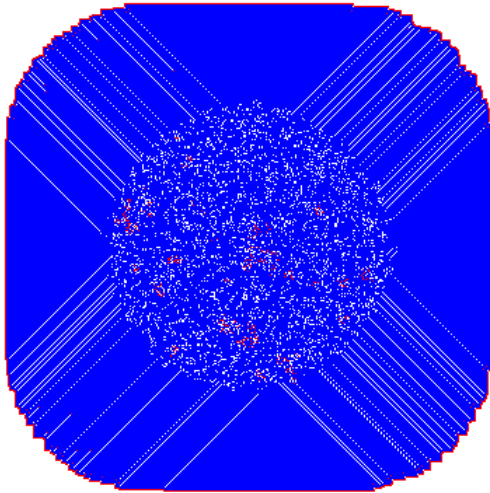
In response D -stimulation automata from these classes generate circular waves of excitaton (Fig. 3ab). The domain D of initial perturbation is a random pattern of refractory and resting states. No excitation is observed inside D in automata from class C_6 and usually just few localised oscillating excitations in automata from C_5 . The circular wave-front leaves behind an almost uniform field of refractory cells with radial traces of resting states towards north-west, north-east, south-west and south-east directions (Fig. 3ab). Functions from classes C_5 and C_6 are positioned close to class C_2 in Fig. 2 due to high ratio of refractory states in configurations they generate. The class C_5 has four functions $\mathcal{M}(1a22)$, $a = 3, \dots, 6$ and the class C_6 has six functions $\mathcal{M}(1abc)$, $a = 7, 8$, $b = 1, 2$, $b \leq c \leq 2$.

2.11. Classes C_7 and C_8

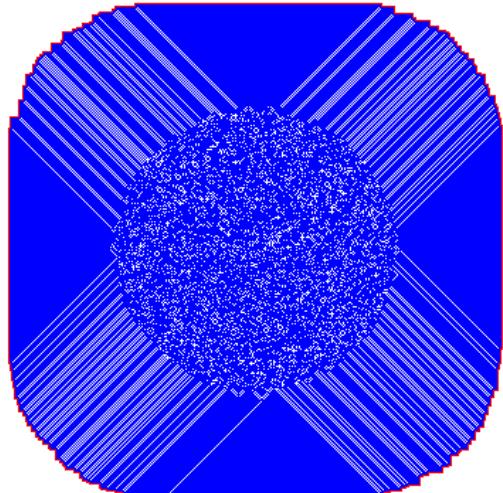
Automata from these classes generate a single circular excitation wave while perturbed by D and a domain of refractory and resting states inside boundaries of D . In automata from C_8 a propagating excitation wave leaves a trail of refractory states along north-west-south-east and north-east-south-west axis, the rest of cells remain in the resting state. Propagating wave-front leaves no traces in automata from C_8 (Fig. 3cd). Class C_7 has 16 functions $\mathcal{M}(1a1b)$, $a = 7, 8$, $b = 3, 4$; $\mathcal{M}(1a2b)$, $a = 7, 8$, $b = 3, \dots, 8$; and, class C_8 has eight functions $\mathcal{M}(1a1b)$, $a = 7, 8$ and $b = 5, \dots, 8$.

2.12. Class C_9

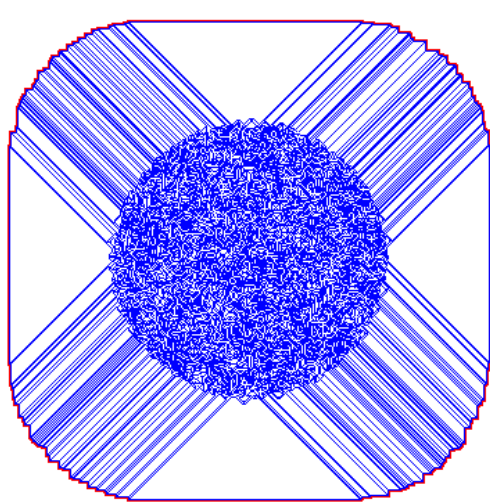
D -stimulation of an automaton from C_9 produces a domain of refractory and resting states (inside boundaries of D) and localizations travelling along north-south and west-east axis (Fig. 4a). The localizations leave traces of refractory states. Configurations produced by functions from C_9 has the lowest (amongst all other classes) ratio of excited states (Fig. 2, C_9). The class C_9 has 17 functions $\mathcal{M}(22ab)$, $a = 1, 2$, $a \leq b \leq 8$; $\mathcal{M}(2a11)$, $a = 3, 4$.



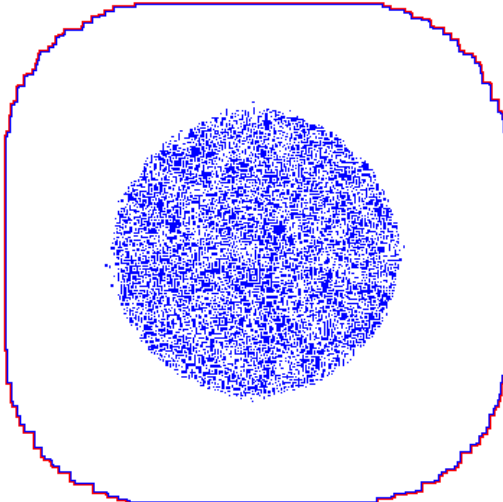
(a) C_5



(b) C_6



(c) C_7



(d) C_8

Figure 3: Exemplars of configurations generated by functions from classes $C_5 \dots C_8$ with D -stimulation. Excited cells are red (light grey), refractory cells are blue (dark grey) and resting cells are white.

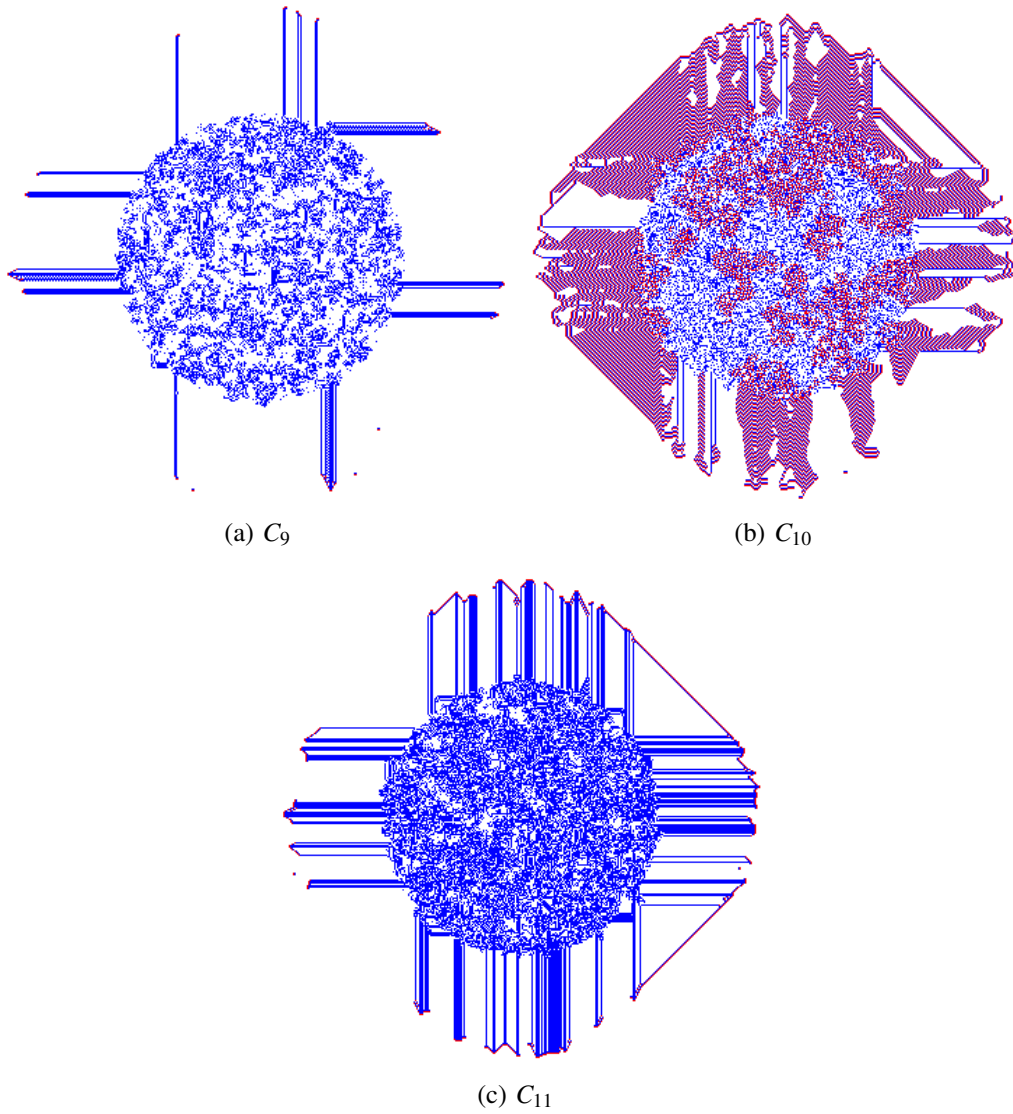


Figure 4: Exemplars of configurations generated by functions from classes $C_9 \dots C_{11}$ with D -stimulation. Excited cells are red (light grey), refractory cells are blue (dark grey) and resting cells are white.

| Class | Shannon entropy | Simpson's index | Space-filling ratio | Expressiveness |
|----------|-----------------|-----------------|---------------------|----------------|
| C_1 | 7.01 | 1.0 | 0.94 | 7.41 |
| C_2 | 5.06 | 0.95 | 0.95 | 5.35 |
| C_3 | 5.99 | 0.96 | 0.96 | 6.24 |
| C_4 | 5.55 | 0.98 | 0.96 | 5.8 |
| C_5 | 1.79 | 0.53 | 0.96 | 1.87 |
| C_6 | 2.15 | 0.65 | 0.96 | 2.23 |
| C_7 | 3.95 | 0.96 | 0.42 | 9.5 |
| C_8 | 4.56 | 0.99 | 0.15 | 31.21 |
| C_9 | 3.89 | 0.95 | 0.14 | 27.69 |
| C_{10} | 5.20 | 0.98 | 0.60 | 8.7 |
| C_{11} | 4.27 | 0.97 | 0.27 | 15.71 |

Figure 5: Average values of Shannon entropy, Simpson's index, space-filling ratio and expressiveness with D -stimulation.

2.13. Class C_{10}

Phenomenology of automata's behaviour is richest amongst all classes. D -stimulation leads to formation of trains of excitation wave-fragments, propagating in north-west, north-east, south-west and south-east directions; domains of localised excitations inside boundaries of D , travelling localizations with and without traces of refractory states (Fig. 4b). Typically excited cells are in slight majority in configurations generated by automata from C_{10} (Fig. 2, C_{10}). The class C_{10} includes 61 functions $\mathcal{M}(2a1b)$, $a, b = 3, \dots, 8$; $\mathcal{M}(2a2b)$, $a, b = 4, \dots, 8$.

2.14. Class C_{11}

Behaviour of automata from class C_{11} is somewhat similar to that of class C_9 but sometimes localizations travelling along north-south and west-east axis are 'linked' by segments from excitation wave-fronts (Fig. 4c). The class C_{11} has 27 functions $\mathcal{M}(2312)$; $\mathcal{M}(232a)$, $a = 2, \dots, 8$; $\mathcal{M}(2412)$; $\mathcal{M}(242a)$, $a = 2, 3$; $\mathcal{M}(2abc)$, $a = 5, \dots, 8$, $b = 1, 2$, $b \leq c \leq 3$.

3. Hierarchies

Finding 1. *Classes of excitable cellular automata with retained refractoriness obey the following power hierarchy:*

$$C_4 \triangleright C_{10} \triangleright \{C_1, C_{11}\} \triangleright C_7 \triangleright C_9 \triangleright \{C_3, C_8\} \triangleright C_6 \triangleright C_5 \triangleright C_2.$$

This is a direct consequence of our joining functions into classes.

Finding 2. *Classes of excitable cellular automata with retained refractoriness obey the following hierarchy of space-filling ratio:*

$$\{C_1, C_2, C_3, C_5, C_6\} \triangleright C_{10} \triangleright C_7 \triangleright C_{11} \triangleright \{C_8, C_9\}$$

Space-filling ratio values averaged amongst each class are shown in Fig. 5 and the distribution of functions inside each class in Fig. 6. Classes C_1 to C_6 , and C_8 show small variance in space-filling ratio while class C_{11} shows largest variance. Roughly the classes can be split into two space-filling groups: high space-filling ratio (C_1, \dots, C_6) and low space-filling ratio (C_7, \dots, C_{11}).

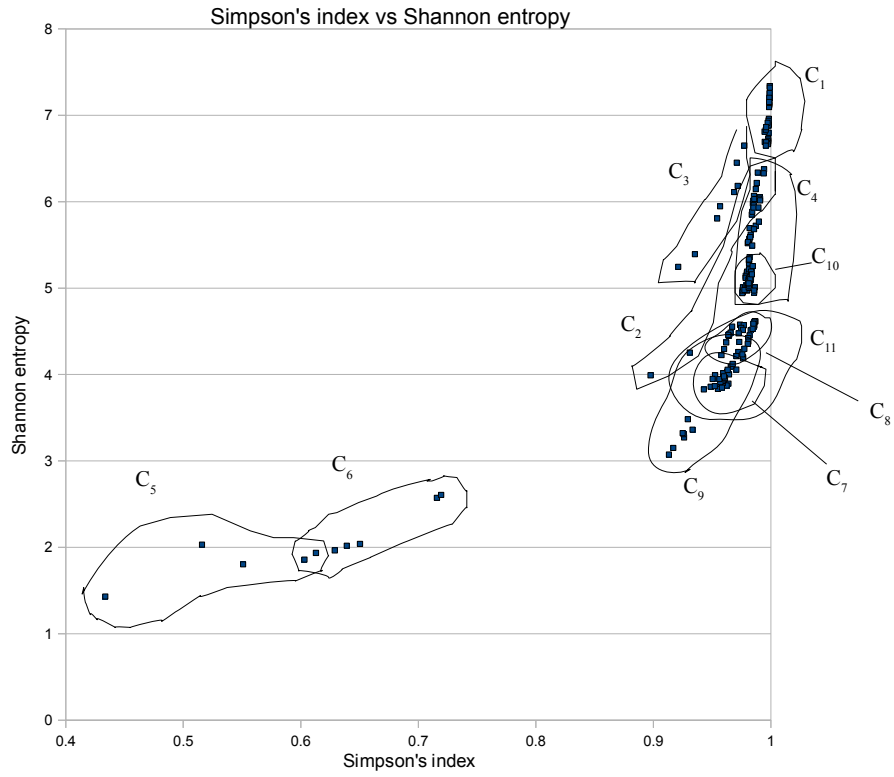
Finding 3. *Classes of excitable cellular automata with retained refractoriness obey the following hierarchy of diversity:*

$$C_1 \triangleright C_3 \triangleright C_4 \triangleright C_{10} \triangleright C_2 \triangleright C_8 \triangleright C_{11} \triangleright C_7 \triangleright C_9 \triangleright C_6 \triangleright C_5.$$

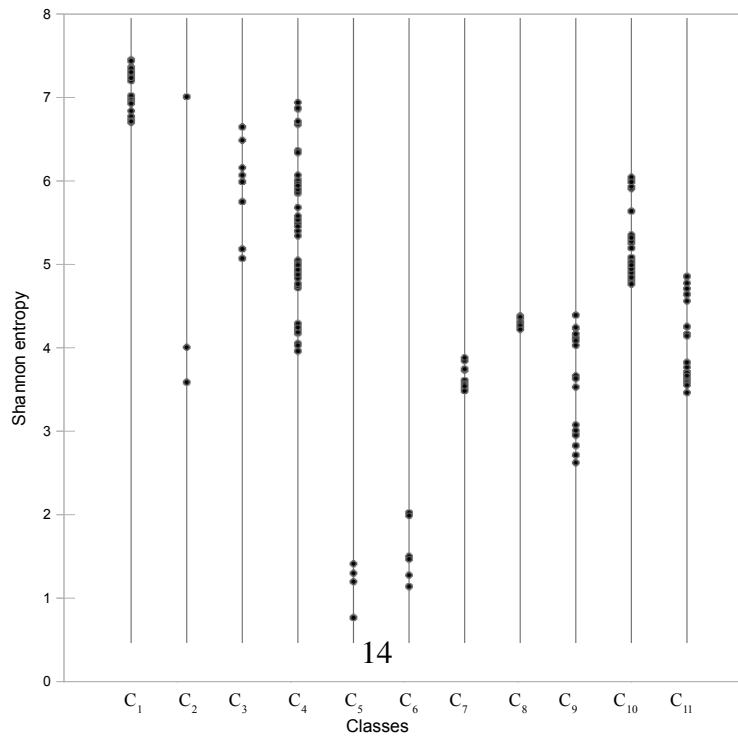
We can draw an analogy between neighbourhood states in a given configuration of cellular automaton and living species in a population. Thus we can measure a diversity of a function by calculating Simpson's index and Shannon entropy of a population of neighbourhood states in a single configuration generated by the function (Fig. 7). Classes C_5 and C_6 exhibit the lowest diversity because initial random excitation pattern D extinguishes quickly and only single propagating wave-front travels away from the site of original excitation. The front leaves behind an almost homogeneous domain of refractory states. Classes C_1 , C_3 and C_4 hold top ranks in the diversity hierarchy because the initial random patterns expands into a growing quasi-random configuration of excited and refractory states. In terms of Shannon entropy class C_3 shows higher degree of diversity than class C_4 (Fig. 5), possibly, because space-time dynamics is biased towards formation of extended wave-fronts propagating north, south, east and west, which interact with fragmentary wave-patterns travelling north-west, north-east, south-west and south-east. Class C_{10} , which demonstrates high variety of travelling localizations, and stays just above the middle of the diversity hierarchy.

Finding 4. *Classes of excitable cellular automata with retained refractoriness obey the following hierarchy of expressiveness:*

$$C_8 \triangleright C_9 \triangleright C_{11} \triangleright C_7 \triangleright C_{10} \triangleright C_1 \triangleright C_3 \triangleright C_4 \triangleright C_2 \triangleright C_6 \triangleright C_5.$$



(a)



(b)

Figure 7: Distribution of classes on morphological diversity. (a) Simpson's index vs Shannon entropy and (b) Shannon entropy with D -stimulation.

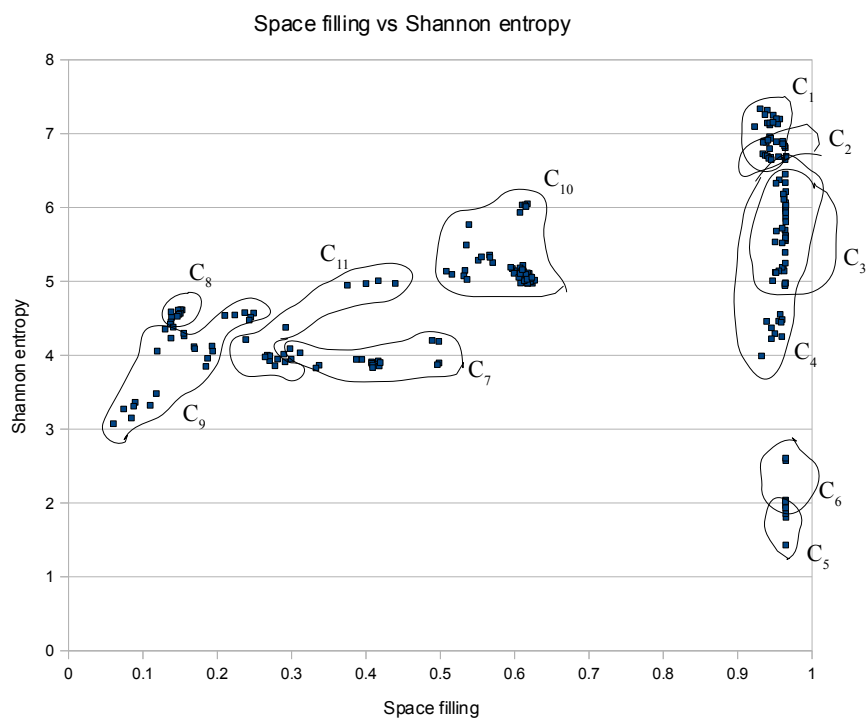


Figure 8: Space-filling ratio vs Shannon entropy with D -stimulation.

Distribution of functions in a space filling versus Shannon entropy space is shown in Fig. 8. Despite having below average diversities classes C_8 and C_9 occupy top level of the expressivness hierarchy. This is because their space filling demands are incredibly modest. Apart of a random refractory domain left after D -perturbation, we observe only propagating excitation wave-front in C_8 and trace leaving localizations in C_9 . They are followed by C_{11} . Automata from C_{11} exhibit varieties of localised and spatially extended excitations.

Finding 5. *Classes of excitable cellular automata with retained refractoriness obey the following hierarchy of generative diversity:*

$$C_1 \triangleright C_2 \triangleright C_9 \triangleright C_{11} \triangleright C_{10} \triangleright C_7 \triangleright C_4 \triangleright C_8 \triangleright \{C_3, C_5, C_6\}.$$

Average values of Shannon entropy of configurations generated by point-wise excitation are shown in Fig. 11. Classes C_1 and C_2 are at the top of generative diversity hierarchy. Typical configurations developed after a point-wise excitation include almost-rectangular patterns (Fig. 9a) and rectangular patterns with 2/3 diamond corners (Fig. 9b). These patterns are symmetric yet sophisticated in terms of visual complexity patterns of excited and refractory states.

In the descending order of generative diversity, classes C_1 and C_2 are followed by classes C_9 and C_{11} . Patterns generated in the result of point-wise stimulation include

- Sierpinski carpets expanding north and south from longest sides of two-cell point-wise excitation (Fig. 10a);
- rhomboid excitation wave fronts, followed by travelling localizations and leaving behind a domain of disordered sparsely distributed refractory states (Fig. 10b);
- rhomboid wave-fronts forming ordered strips of refractory states (Fig. 10cd);
- and combinations of localised and spatially-extended refractory-state domains (Fig. 10ef).

Class C_{10} occupies a mid-range of generative diversity. A point-wise excitation generates rhomboid patterns of wave packets, each excitation front is followed by a refractory tail (Fig. 9cd). Some functions of the class also produce a narrow band of resting states, surrounded by excitation domain (Fig. 9c). Classes C_3, C_5, C_4, C_6, C_8 have lowest generative diversity. A point-wise excitation leads to formation of a circular excitation wave, which leaves a trail of refractory states.

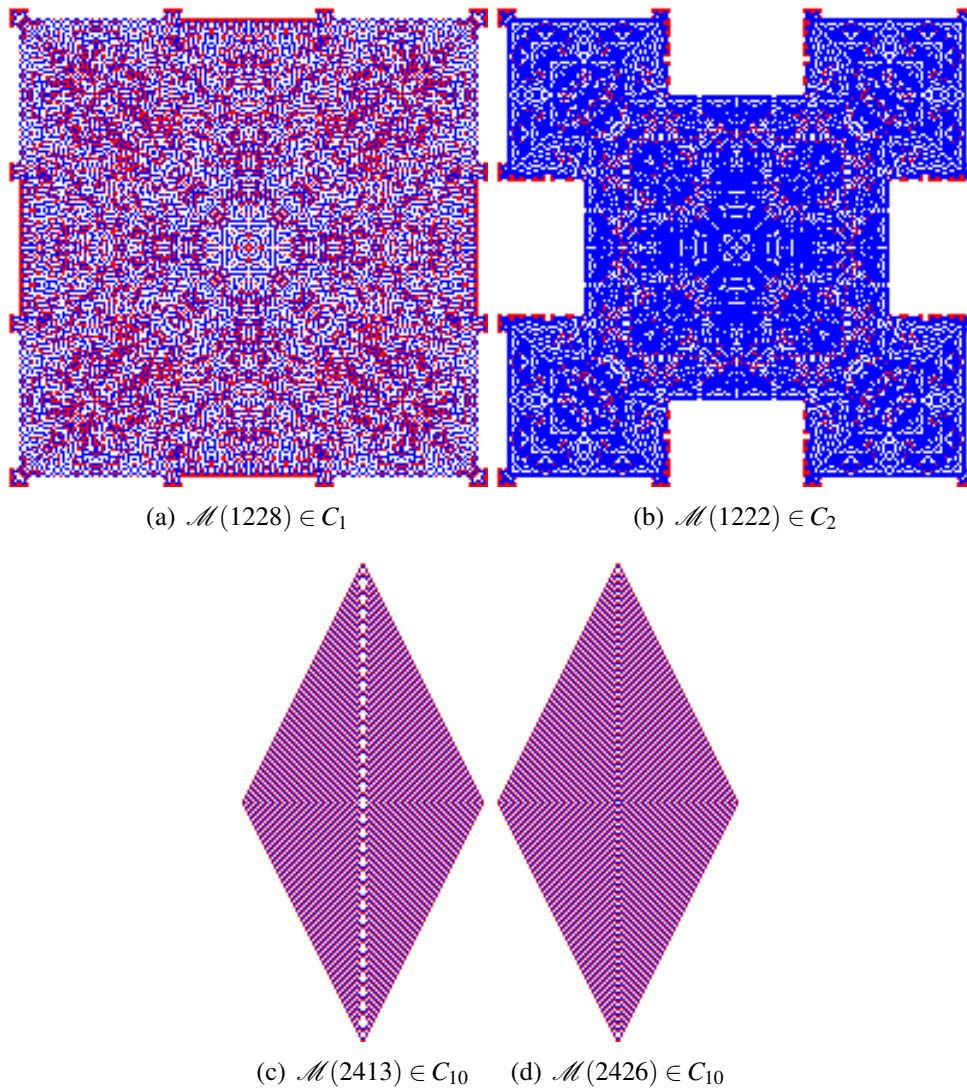


Figure 9: Typical configurations, developed after point-wise excitation, generated by functions (a) C_1 , (b) C_2 , (cd) C_{10} . Names of functions are indicated in the sub-captions. Snapshots of configurations are taken 100 time steps after point-wise perturbation. Excited cells are red (light grey), refractory cells are blue (dark grey) and resting cells are white.

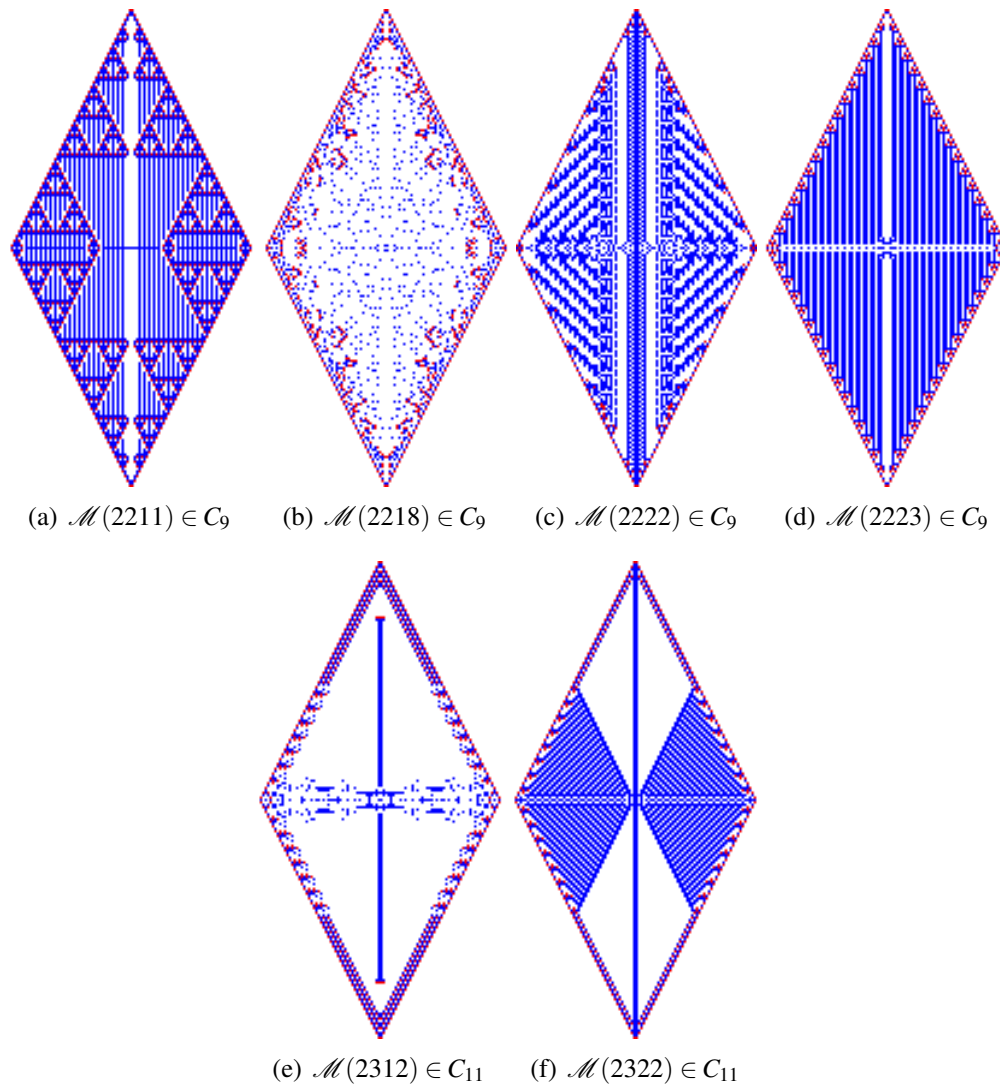


Figure 10: Typical configurations, developed after point-wise excitation, generated by functions (a–d) C_9 , and (ef) C_{11} . Exact functions are indicated in the sub-captions. Snapshots of configurations are taken 100 time steps after point-wise perturbation. Excited cells are red (light grey), refractory cells are blue (dark grey) and resting cells are white.

| Class | Shannon entropy | Simpson's index | Space-filling ratio | Expressiveness |
|----------|-----------------|-----------------|---------------------|----------------|
| C_1 | 6.89 | 1.0 | 0.90 | 7.65 |
| C_2 | 5.52 | 0.98 | 0.84 | 6.6 |
| C_3 | 0.31 | 0.10 | 1.0 | 0.31 |
| C_4 | 2.86 | 0.94 | 0.08 | 34.32 |
| C_5 | 0.31 | 0.1 | 1.0 | 0.31 |
| C_6 | 0.31 | 0.1 | 1.0 | 0.31 |
| C_7 | 2.93 | 0.94 | 0.09 | 32.58 |
| C_8 | 2.71 | 0.93 | 0.07 | 38.79 |
| C_9 | 4.55 | 0.96 | 0.22 | 20.59 |
| C_{10} | 3.16 | 0.94 | 0.27 | 11.71 |
| C_{11} | 3.80 | 0.95 | 0.21 | 17.91 |

Figure 11: Average values of Shannon entropy, Simpson's index, space-filling ratio and expressiveness calculated on configurations generated by a point-wise excitation.

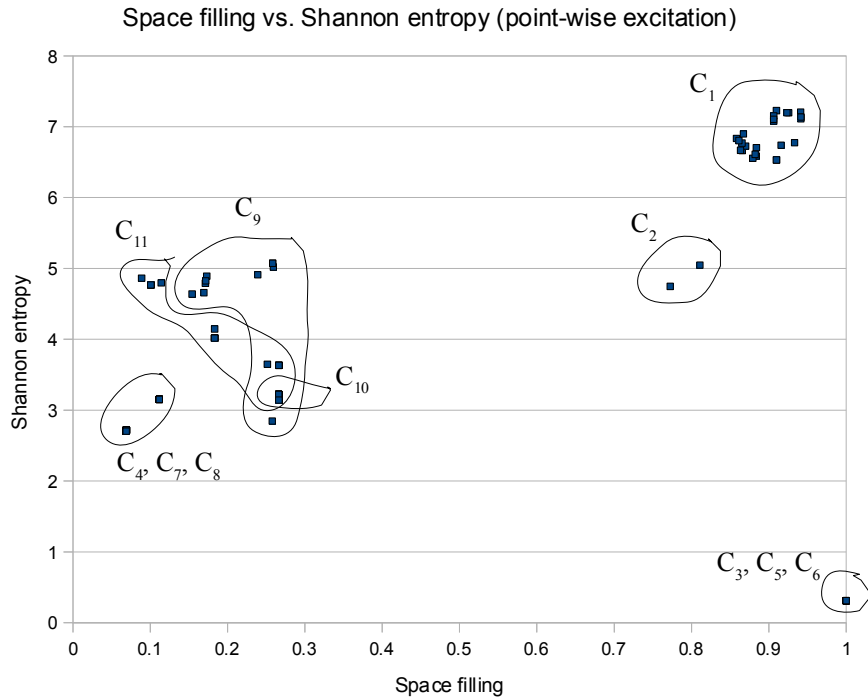


Figure 12: Space-filling ratio vs Shannon entropy. Point-wise excitation.

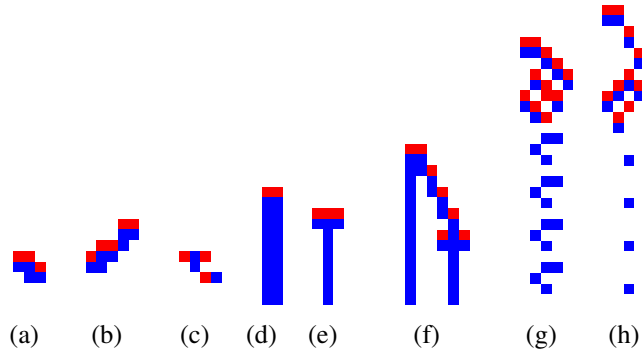


Figure 13: Examples of travelling localizations found in configurations of automata with retained refractoriness. (a–e) Gliders, (f–h) Trains. Excited cells are red (light grey), refractory cells are blue (dark grey) and resting cells are white.

Finding 6. *Classes of excitable cellular automata with retained refractoriness obey the following hierarchy of generative expressiveness:*

$$C_8 \triangleright C_4 \triangleright C_7 \triangleright C_9 \triangleright C_{11} \triangleright C_{10} \triangleright C_1 \triangleright C_2 \triangleright \{C_3, C_5, C_6\}.$$

See detailed structure of the hierarchy in Fig. 12.

4. Travelling localisations

Travelling localised excitations is a unique phenomenon of sub-excitable media, widely used in theoretical and experimental laboratory implementations of novel computing architectures, see e.g. [4]. Most common localizations found in experiments with excitable automata with retained refractoriness are gliders, trains, glider guns, and spaceships. These structures are well-known in Conway’s Game-of-Life cellular automata (and we are using terminology of the Conway’s Game of Life) however they display a range of uncommon properties when inhabiting discrete excitable medium.

Examples of gliders (localizations which do not leave traces) and trains (localizations which leave traces made of stationary refractory patterns) are shown in Fig. 4; all localizations shown there travel north. A glider shown in Fig. 4a consists of three excited and states. The small gliders can be joined together to make propagating wave-fragments: in Fig. 4b we see a glider made of three excited and three refractory states joined with a localisation of two excited and two refractory states. The gliders move along columns and rows of a cellular array. Similarly

to our previous models of sub-excitable discrete media, e.g. [4], we found only one excited localisation which travels along diagonals of the cellular array. The diagonal glide consists of three excited and three refractory states, an exemplar snapshot is shown in Fig. 4c.

Gliders which leave traces of stationary patterns behind are called trains. The trains are very common in classes C_9 , C_{10} and C_{11} . A minimal train consists of a pair of excited states leaving a column/row of refractory pairs behind (Fig. 4d). In terms of trace minimality, the train shown in Fig. 4e is minimal localisation of three excited states which leaves a trace of refractory states one-cell wide. Trains can be linked with gliders and other trains, an example is shown in (Fig. 4f). Trains leaving localised traces of refractory states are shown in (Fig. 4gh).

Travelling localizations which generate streams of other localizations, e.g. gliders, are called mobile guns (Fig. 14). A mobile gun can emit localisation in any directions, subject to the lattice's discreteness, apart of the direction of the gun's motion. Here we illustrate just few examples: gun travels east and emits trains travelling south (Fig. 14a), gun travels east and emits gliders travelling west (Fig. 14b), gun travels north and emits trains travelling east (Fig. 14c), gun travels north and emits gliders travelling west (Fig. 14d). A complex gun is shown in (Fig. 14e): the gun travels north and emits three streams of gliders, one stream travels west and two streams travel east.

Interactions between gliders is pretty rich, gliders and trains can reflect or annihilate in the result of the collision, also refractory stationary patterns can be formed in the results of such collisions. An example is shown in Fig. 15. Two mobile guns travel north. They both leave a trace of refractory states, as trains do. Westward gun emits a single stream of gliders travelling east. Eastward gun emits two streams of gliders. Eastward stream of westward gun collides with westward stream of eastward gun. Refractory patters are formed in the result of collision, and glider streams are pruned: only every fifth glider of westward stream survives collision and only every fourth glider of eastward stream survives the collision (Fig. 15).

Functions $\mathcal{M}(2a1b)$, where $a = 3, \dots, 8$ and $b = 1, 2$, generate spaceships ($b = 1$) and Sierpinski flying carpets ($b = 2$). Sierpinski carpets and spaceships observed in many types of cellular automata including Conway's Game of Life [19, 16]. However, we believe, travelling Sierpinski carpets have never been observed before in cellular automata. Examples of Sierpinski carpets generated by function $\mathcal{M}(2311)$ from seeds of different sizes are shown in Fig. 16. The carpets always leave a trail of refractory states. Therefore they can be considered as analogies of puffer trains [15] in the Game of Life cellular automata.

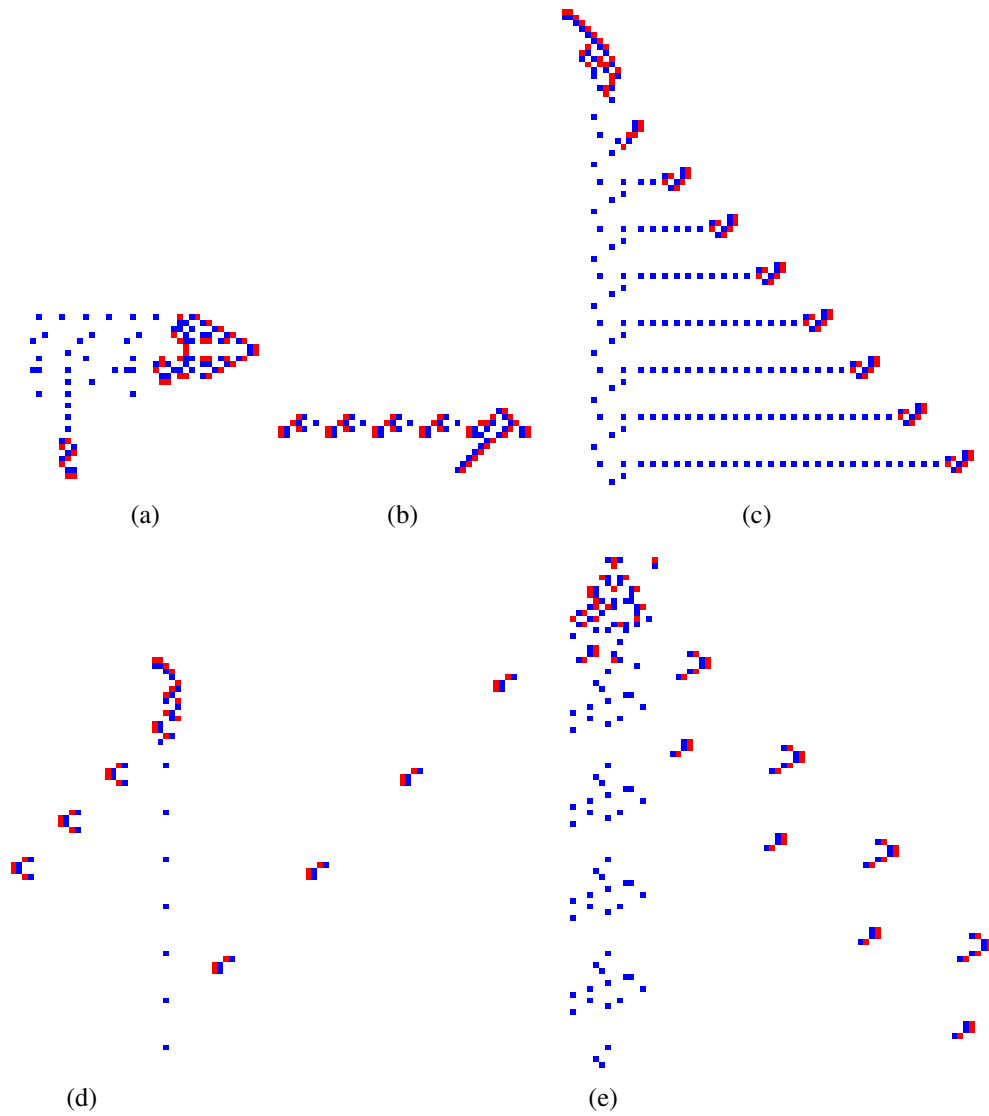


Figure 14: Examples of mobile glider guns found in development of automata with retained refractoriness. Excited cells are red (light grey), refractory cells are blue (dark grey) and resting cells are white.

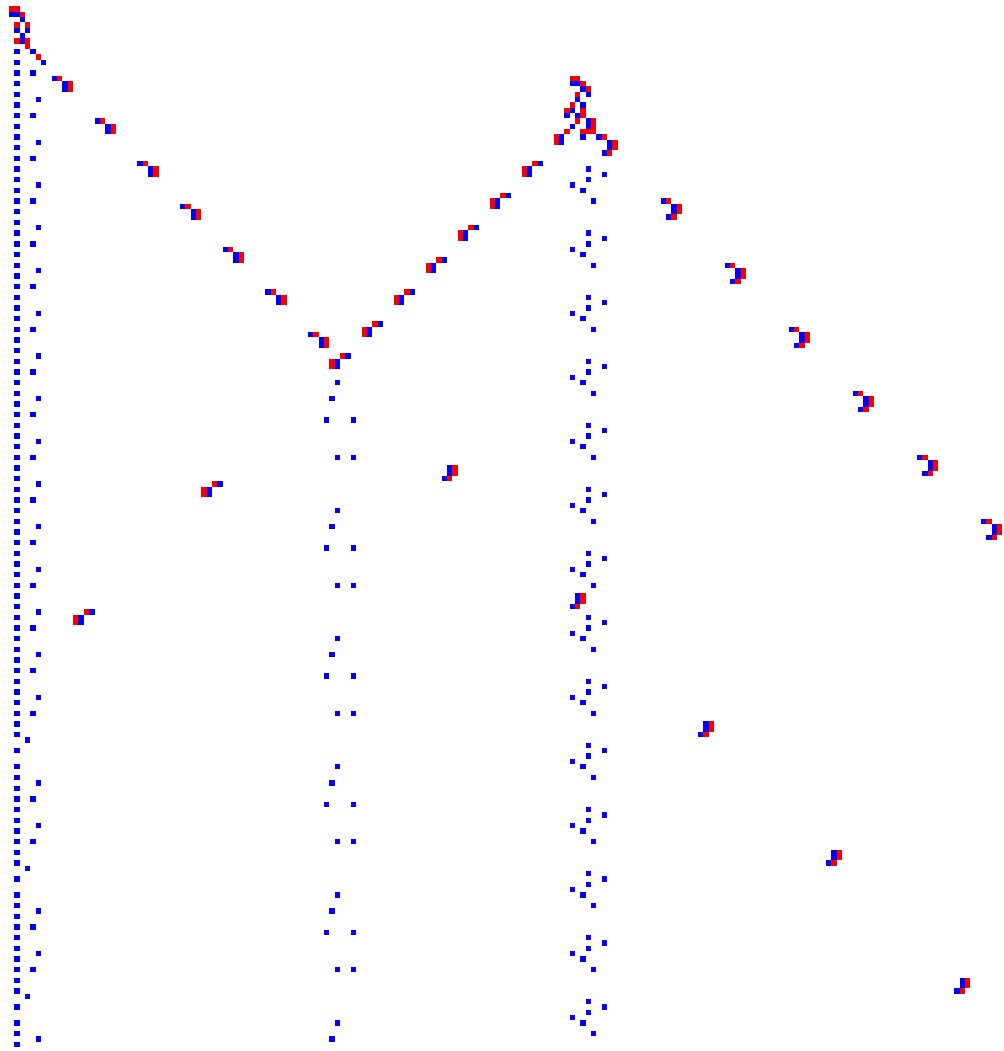


Figure 15: Example of interactions between travelling excitations in automata with retained refractoriness. Excited cells are red (light grey), refractory cells are blue (dark grey) and resting cells are white.

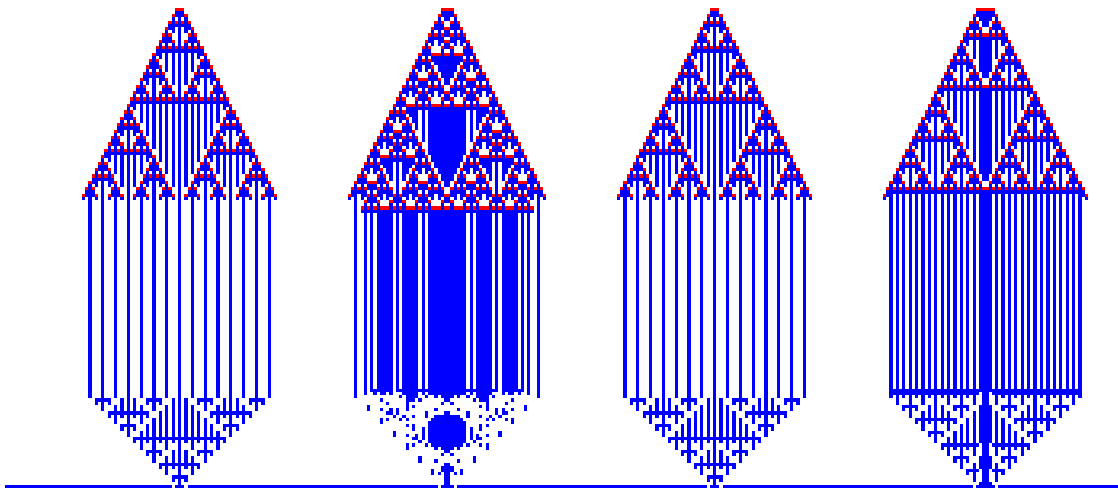


Figure 16: 'Flying' Sierpinski carpets, generated by automata of class C_9 . Carpets travel north. Patterns (from the left to the right) are generated by lines of two, three, four and five excited cells. Launching pad is constructed by a glider, which travels east and leaves a refractory trail. The configurations are generated by function $\mathcal{M}(2311)$. Excited cells are red (light grey), refractory cells are blue (dark grey).

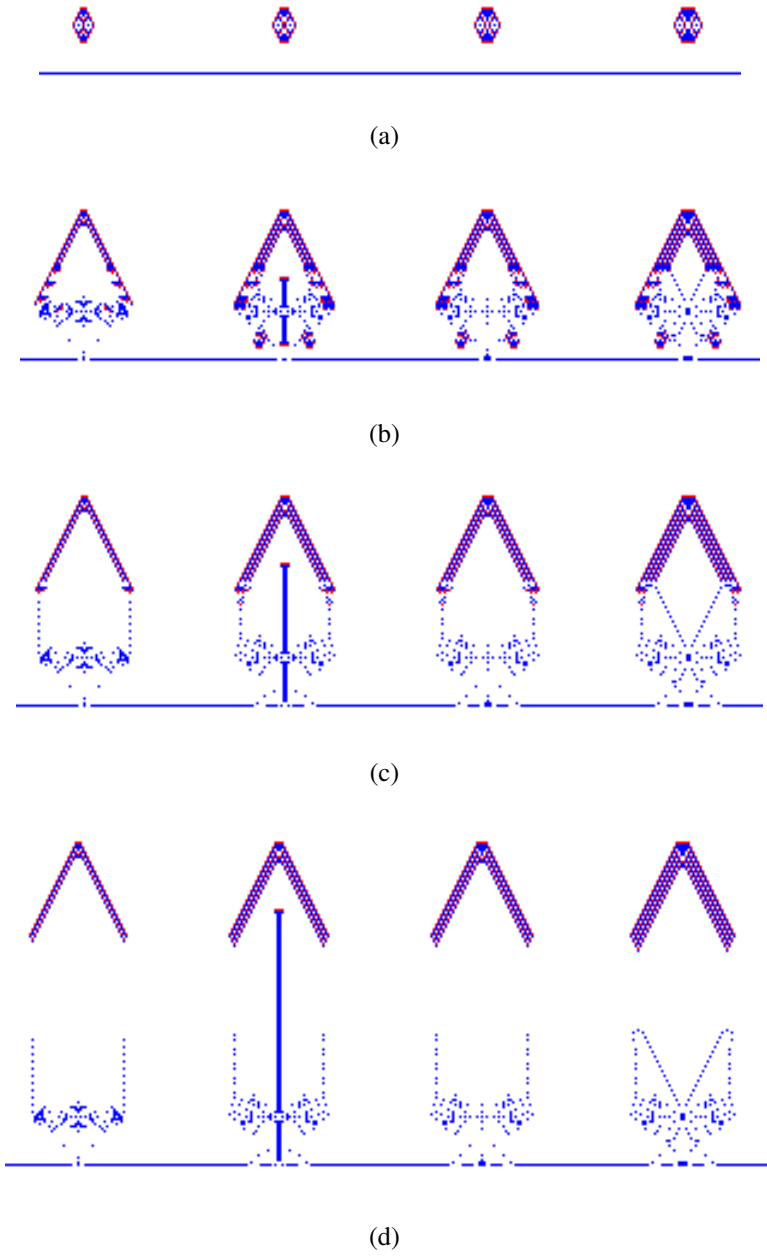


Figure 17: Formation and propagation of spaceships in automata of class C_{11} . Patterns (from the left to the right) are generated by lines of two, three, four and five excited cells. Launching pad is constructed by glider travelling east and leaving refractory trail. (a) Generation stage. (bc) Take-off stage. (d) Flying. The configurations are generated by function $\mathcal{M}(2312)$. Excited cells are red (light grey), refractory cells are blue (dark grey).

Spaceships do not leave refractory debris behind. Several stages of spaceships development are illustrated in Fig. 17. A strip of excited states, e.g. '+' , ''++' , ''+++ ' etc., leads to formation of self-similar growing rhomb (Fig. 17a and Fig. 10ae). When the south part of the rhomb gets in touch with a refractory strip it becomes 'infected' with refractory states, or frozen, thus only north part of the rhomb continues travelling (Fig. 17bc). At some stage a spaceship becomes disconnected from refractory debris it left and gets 'airborne' (Fig. 17d).

Both Sierpinski flying carpets and spaceships observed are rather close relatives of 'grayships' [16], because they are comprised of still patterns which can be extended to arbitrary size. The size of each carpet or spaceship is determined by the distance of its seed from the launchpad (a chain of refractory states, which prevents the carpet/spaceship from expanding in one direction).

Collisions between the flying carpets and spaceships develop along 'classical' scenarios of collisions between travelling localizations: annihilation and reflection, possibly with emergence of new localizations (Fig. 18).

5. Discussion

Aiming to design a cellular automaton model of a discrete memristive medium we developed a model of excitable cellular automaton with retained refractoriness. The model is ideologically similar to our previous model of cellular automata with retained excitation [5] but the focus shifted to retained refractoriness. An excited cell takes refractory state unconditionally, i.e. independently of the number of its excited neighbours, however the refractory cell can remain in its refractory state depending on the number of its excited neighbours.

A propagation of excitation in a medium can be considered as an analog of electrical current. A refractory state is an automaton analog of high-resistance state of a memristive element, and a switching from the refractory state to resting state, controlled by a density of local excitation, is an analog of switching the memristive element to its state of low-resistance. The automata studied are semi-memristive because switching from low-resistance (resting) state to high-resistance (refractory) state is not controlled by electrical current (density of local excitation).

Classical automaton models of excitable media are usually based on the principle of threshold excitation: a resting cell excites if the number of excited neighbours exceeds certain threshold. This threshold-view on excitation dynamics was the main reason why mobile localizations have not been discovered for so long time. In [1] we introduced interval-based excitation: resting cell takes excited

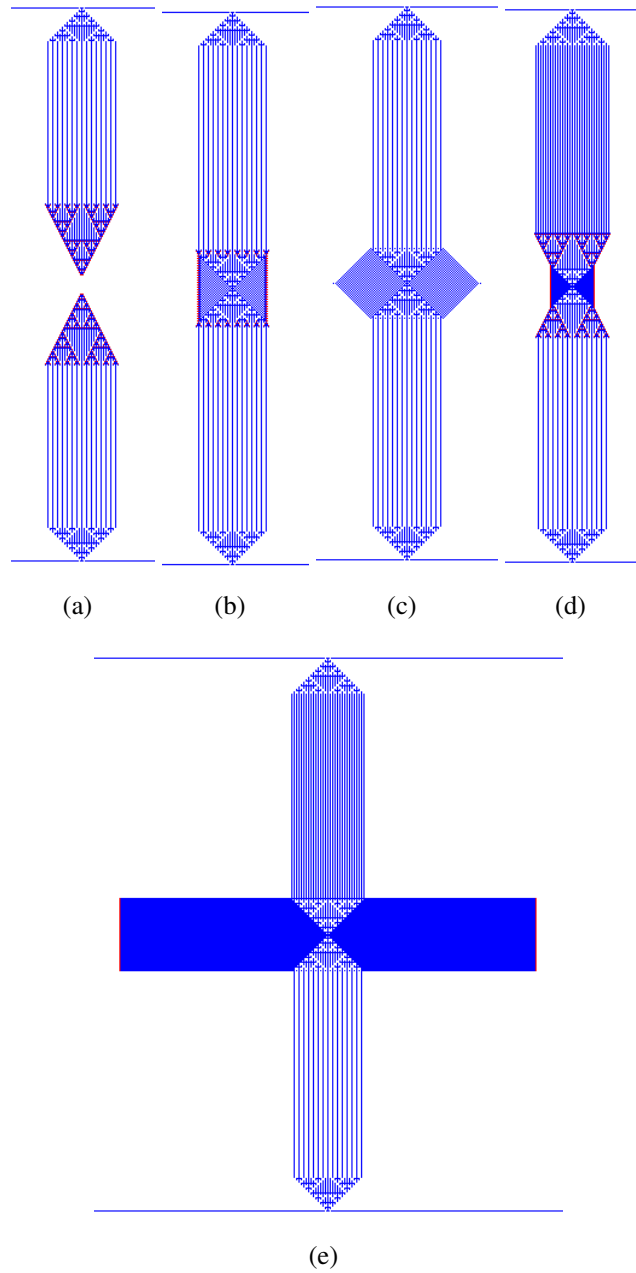


Figure 18: Interaction of flying Sierpinski carpets in automata of class C_{11} . (a) Carpets approach each other. (bc) Even distance: (b) full body impact and (c) formation of debris/annihilation. (de) Odd distance: (d) full body impact and (e) formation of new travelling localizations. The configurations are generated by function $\mathcal{M}(2811)$; seed's size is two cells; distance of a seed from southern refractory strip (launchpad) is 50 cells. Excited cells are red (light grey), refractory cells are blue (dark grey).

state if the number of its excited neighbours belongs to some specified interval. The approach proved to be productive — a range of non-classical computing devices [4], based on the rich phenomenology of excitation in interval-excitation-based models, was designed. Therefore we employed interval-based excitation and also interval-based recovery, i.e. transition from refractory to resting state, to imitate semi-memristive automata.

Based on functions' behavioural grouping, visual categorisation of configurations generated in a response to random perturbation, ordering functions on their morphological diversity and expressiveness we selected eleven classes of functions: C_1, \dots, C_{11} .

The functions of classes C_1, \dots, C_6 show high degree of space-filling ratios, while classes C_7, \dots, C_{11} mid-range and low space-filling ratios. Low space-filling classes can be further sub-divided into classes with extinct excitation, namely C_7 and C_8 , where only a single centripetal wave-front is formed, and classes that support travelling localizations: C_9, C_{10}, C_{11} . The low space-filling classes C_7, \dots, C_{11} also demonstrate higher ratio of excited states over refractory states in configuration functions of the classes generate.

Top four classes in the hierarchy of morphological diversity are C_1, C_3, C_4 and C_{10} . Automata from C_1, C_3 and C_4 show rather quasi-chaotic response to spatially extended random excitation, and this is the reason for their high morphological diversity. Class C_{10} is more interesting. A spatially extended random perturbation leaves a random configuration of refractory states filled with non-expanding, sometimes breathing, domains of localised excitations and a combination of propagating wave-fronts, wave-fragments and travelling localizations.

Top four classes in the hierarchy of generative diversity are C_1, C_2, C_9 and C_{11} . Classes C_1 and C_2 show quasi-chaotic dynamics and even a point-wise excitation of a resting lattice leads to formation of a complex growing pattern. Class C_9 got to the top four of generative diversity because a point-wise excitations give birth to expanding Sierpinski carpets, and disordered and highly-ordered arrangements of refractory states.

To refine our classification even further we introduced a measure of expressiveness, which relates morphological diversity to space-filling ratio, and thus reflects an 'economy of diversity' in cellular automaton configurations. As you can see in Fig. 8, classes C_9, \dots, C_{11} show higher degrees of expressiveness. Thus we can propose that functions which support travelling localizations may be at the mid-range levels of morphological diversity but top levels of expressiveness.

We briefly characterised a range of travelling localizations which emerged in the cellular automata studied. We demonstrated that many localizations are

capable for laying sophisticated patterns of refractory, high-resistive in memristor's terminology, states. Such patterns could be used in further studies to compartmentalise otherwise homogeneous spatially extended memristive media. We found outcomes of collisions between propagating localisation are quite rich and therefore all scenarios of collision-based computing [3] can be implemented in semi-memristive cellular automata. Our further studies will be concerned with developing fully memristive cellular automaton model and designing laboratory experimental prototypes of large-scale memristive media.

Bibliography

References

- [1] Adamatzky A. and Holland O. Phenomenology of excitation in 2D cellular automata and swarm systems, *Chaos, Solitons & Fractals* 3 (1998) 1233–1265.
- [2] Adamatzky A. *Computing in Nonlinear Media and Automata Collectives* (IoP Publishing, London, 2001).
- [3] Adamatzky A. (Ed.) *Collision Based Computing* Springer, 2003.
- [4] Adamatzky A., De Lacy Costello B., Asai T. *Reaction-Diffusion Computers* (Elsevier, Amsterdam, New York, 2005).
- [5] Adamatzky A. Phenomenology of retained excitation. *Int J Bifurcation and Chaos* 17 (2007) 3985–4014.
- [6] Adamatzky A. and Chua L. Memristive excitable cellular automata. *Int. J. Bifurcation Chaos* (2011), in press.
- [7] Chua L. O., Memristor — the missing circuit element. *IEEE Trans. Circuit Theory* 18 (1971) 507–519.
- [8] Chua L. O. and Kang S. M., Memristive devices and systems. *Proc. IEEE* 64 (1976) 209–223.
- [9] Chua L. O. Device modeling via non-linear circuit elements. *IEEE Trans. Circuits Systems* 27 (1980) 1014–1044.
- [10] Erokhin V., Fontana M.T. Electrochemically controlled polymeric device: a memristors (and more) found two years ago. (2008) arXiv:0807.0333v1 [cond-mat.soft]
- [11] Halpern P. and G. Caltagirone. Behavior of topological cellular automata. *Complex Systems* 4 (1990) 623651.
- [12] Ilachinsky A. and Halpern P., Structurally dynamic cellular automata, *Complex Systems* 1 (1987) 503–527.

- [13] Itoh M. and Chua L. Memristor cellular automata and memristor discrete-time cellular neural networks. *Int. J. Bifurcation and Chaos* 19 (2009) 3605–3656.
- [14] Greenberg J. M. and Hastings S. P. Spatial patterns for discrete models of diffusion in excitable media, *SIAM J. Appl. Math.* 34 (1978) 515-523.
- [15] Puffer train. LifeWiki. (2010) http://www.conwaylife.com/wiki/index.php?title=Puffer_train
- [16] Spaceship. LifeWiki. (2010) <http://www.conwaylife.com/wiki/index.php?title=Spaceship>
- [17] Strukov, D.B., Snider, G. S., Stewart, D. R. and Williams, R. S., The missing memristor found. *Nature* 453 (2008) 80–83.
- [18] Williams R. S. How we found the missing memristor. *IEEE Spectrum* 2008-12-18.
- [19] Wisialowski B. Conways Game of Life: Lines to Fractals <https://webfiles.uci.edu/bwisialo/www/gameoflife2.html>
- [20] Yang, J.J., Pickett, M. D., Li, X., Ohlberg, D. A. A., Stewart, D. R. and Williams, R.S. Memristive switching mechanism for metal-oxide-metal nanodevices. *Nature Nano*, 2008 3(7).